JMEPEG (2019) 28:4316–4323
https://doi.org/10.1007/s11665-019-04182-0

Effects of Particle Characteristic Parameters on the Electrical Conductivity of TiB_2/Cu Composites: A Modified Model for Predicting Their Electrical Conductivity

Jiang Feng, Shuhua Liang, Kexing Song, Xiuhua Guo, Yi Zhang, Guohui Li, and Alex A. Volinsky

(Submitted January 16, 2018; in revised form May 2, 2019; published online July 3, 2019)

High-strength and highly conductive copper matrix composites can not only maintain excellent electrical and thermal conductivity but also enhance the strength and hardness of materials, showing that composites have a bright future for development. Predictions of the effective electrical conductivity of copper matrix composites disagree with experimental data due to the dependence of the composites on several factors. Most prediction models simply consider the influence of the particle volume fraction on conductivity. In the present study, the influence of the volume fraction and the size of the TiB_2 particle on the electrical conductivity of TiB_2/Cu composites are investigated. The obtained electrical conductivity results correlate with the volume fraction, size, and distribution of particles in a pure copper matrix. A modified model for predicting the electrical conductivity is proposed where the particle spacing parameters are introduced into the existing Maxwell model. The particle spacing parameter, as a fitting parameter, fits the experimental data of the copper matrix composites excellently.

Keywords copper matrix composites, effective electrical conductivity, model

1. Introduction

Copper matrix composites offer many uses because they exhibit an excellent combination of electrical and thermal conductivity. However, the applications of pure copper at high temperatures are limited due to its poor mechanical properties (Ref 1-7). However, reinforcement of copper matrix composite with particles not only enhances the mechanical performance but also maintains the desirable thermal and electrical conductivity of copper (Ref 6, 8-11). However, several factors influence the electrical conductivity of copper matrix composites, including the volume fraction, size, interfacial bonding state, and distribution of the reinforcing particles. Although optimal performance can be obtained by adjusting the preparation parameters, the experimental setup is costly and requires a great deal of effort. Modeling, however, is an appropriate substitution method for promoting the experimental procedures.

Over the past 100 years, several models have been used to predict the electrical conductivity of metal matrix composites. Maxwell was the first to obtain an expression for the effective electrical conductivity of composites based on electrostatic theory that satisfies the Laplace equation. This approximation considers a dilute volume fraction in the model (Ref 12, 13). Rayleigh assumes that the reinforcing phase is spherical or cylindrical and uniformly distributed in the matrix and that the electrical conductivity of the reinforcing phase and matrix is of the same order of magnitude (Ref 14). Roig and Schoutens (Ref 15-17) developed a general theory for alloy electrical conduction at cryogenic and higher temperatures. Bruggeman's model can be used to calculate the electrical conductivity of particle-reinforced metal matrix composites with a high-volume fraction (Ref 18). Frank et al. (Ref 19) proposed a model that considers the combined electrical conductivity of both the matrix and the reinforcements. This theory considers the volume fraction and the geometric arrangement of the reinforcements. The Hashin composite spheres model can also predict the conductivity of metal matrix composites (Ref 20, 21); however, the particle size is not taken into account.

The aforementioned electrical conductivity models for metal matrix composites are based on the electrical conductivity of the matrix and the reinforcements and the volume fraction of the reinforcements. However, these models do not account for the effect of particle size and the interfacial bonding state on electrical conductivity; in some cases, substantial deviation from the experimental results is observed. Efe et al. (Ref 1) discovered that particle size affects the electrical conduction of composites. Zhang (Ref 22) and Wang (Ref 23) prepared the ZrB_2/Cu composites and indicated that their electrical conductivity increased with increasing particle size. Guo et al. (Ref 24) studied the effect of the interfacial bonding state on the electrical conductivity of MgO_p/Cu composites and found that the electrical conductivity of composites with an incoherent interface was lower than that with conforming or semiconforming interface.

Jiang Feng and **Shuhua Liang**, School of Materials Science and Engineering, Xi'an University of Technology, Xi'an 710048, China; **Kexing Song, Xiuhua Guo, Yi Zhang,** and **Guohui Li**, School of Materials Science and Engineering, Henan University of Science and Technology, Luoyang 471003, China; and **Alex A. Volinsky**, Department of Mechanical Engineering, University of South Florida, Tampa 33620. Contact e-mails: fhap256@163.com, liangsh@xaut.edu.cn, and kxsong@haust.edu.cn.

Therefore, in the present work, we considered the influence of the particle size and interfacial bonding state on the electrical conductivity. TiB_2-reinforced copper matrix composites were produced by powder metallurgy, and the influence of the particle size and volume fraction of TiB_2 on the material's electrical conductivity was investigated. For the particulate-reinforced copper matrix composites, the particle size, volume fraction, and interfacial bonding state were taken into consideration in the modified model. The predictions of the modified model agree well with experimental results from the literature.

2. Experimental Details

To fabricate the TiB_2/Cu composites containing 1, 3, and 5 vol. % TiB_2, commercial Cu powder (99.9% purity) of 75 μm particle size and TiB_2 powders (99.7% purity) of 10, 50, and 100 μm sizes were used. The powders were mechanically mixed and then pressed into cylinders of ∅80 mm × 60 mm at a pressure of 350 MPa. The samples were then sintered at 950 °C for 1 h in a bell-type furnace under hydrogen. The sintered samples were hot-extruded into ∅18 mm rods at 900 °C and 840 MPa. The samples were then mechanically ground, polished, and etched with a corrosive agent (3 g $FeCl_3$, 2 mL HCl, and 95 mL C_2H_5OH) for metallographic examination. Microstructural analysis was subsequently conducted using a metallographic microscope (Axio Vert A1). The morphologies and sizes of the Cu and TiB_2 particle were examined using a scanning electron microscope equipped with an energy-dispersive spectrometer (SEM and EDS, JSM-5610LV). The particle size was evaluated with a laser particle size analyzer (LS-909). The electrical conductivity of each sample was determined using a digital conductivity meter (Sigma 2008B1).

3. Results and Discussion

3.1 Microstructure

Figure 1 illustrates the SEM microstructure of the copper and TiB_2 powders and size distributions of the TiB_2 powders. Figure 2 illustrates an optical micrograph of the polished surfaces of the hot-extruded composites reinforced with TiB_2 particles of different sizes and content amounts. Figure 2 shows that the gray particles are TiB_2 and are homogeneously dispersed in the copper matrix without any agglomeration. In the hot-extrusion process, the agglomerated TiB_2 particles can be dispersed uniformly because of the rapid flow of copper matrix, and the pores in the copper matrix can also be filled rapidly. Both factors can lead to an increase in the density and electrical conductivity of the TiB_2/Cu composite. As shown in Fig. 2, the TiB_2 particles distribute uniformly in the copper matrix with a compact microstructure. For composite materials, achieving a homogeneous reinforcement in the matrix is critical to enhance the mechanical, electrical, and thermal properties (Ref 1).

SEM images, the corresponding element mapping images, and EDS lines scans of Cu-5 vol. % 10 μm TiB_2 composites are shown in Fig. 3. Figure 3(a) shows that the composite has a compact structure and that TiB_2 particles are distributed uniformly in the dispersed copper matrix, where the gray particles are TiB_2. The EDS line scans show that no mutual solubility exists between the TiB_2 particles and copper matrix, which confirms the stability of the copper and TiB_2. No interfacial reaction is observed between the TiB_2 and copper matrix. Figure 3(a) also shows fine gaps at the interface between TiB_2 particles and the copper matrix. Therefore, the interface is a mechanical conjunction.

3.2 Electrical Conductivity

The electrical conductivity of the TiB_2/Cu composites is shown in the contour diagram in Fig. 4. The electrical conductivity of the TiB_2/Cu composites can be affected with both the TiB_2 particles volume fraction and its particles size. When the particle size is fixed, the electrical conductivity decreases with increasing volume fraction. This is behavior is attributed to the electrical conductivity of the reinforcing particles being lesser than that of the copper matrix; the introduction of the reinforcing particles into the copper matrix destroys the continuity of the copper matrix and weakens the conductivity of the composites. However, when the particle size nears the micron level, the particle spacing is much larger than the mean free path for electron conduction. In this case, the volume fraction is the predominant factor; thus, the effect of particle size on the electrical conductivity is minor. This hypothesis is confirmed by experimental data. Although the volume fraction is constant, the smaller particle size introduced in the copper matrix means a larger quantity of particles and smaller particle spacing. The metal free-electron theory suggests that a decrease in particle spacing has a weakening effect on the conductivity. Therefore, the electrical conductivity increases with increasing particle size. As shown in Fig. 4, when the volume fraction is constant and the particle size and spacing are small, the decrease in the electrical conductivity of the copper matrix composites is more profound.

Similar varieties of electrical conductivity were found in copper matrix composites reinforced with SiC or ZrB_2 particles. Efe et al. (Ref 1) investigated the effect of the SiC particle size on SiC/Cu composites and showed that the electrical conductivity of the SiC/Cu composites decreases with increasing SiC particle volume fraction and increases with increasing SiC particle size. Zhang (Ref 22) and Wang (Ref 23) investigated the ZrB_2/Cu composites and found that the electrical conductivity also increases with increasing particle size. This effect has once again been proven. Therefore, the electrical conductivity of two-phase composites depends on the volume fraction, the size, and the electrical conductivity of the constituent phases.

3.3 Establishment and Verification of the Electrical Conductivity Model

Maxwell was the first to obtain an expression for the effective electrical conductivity of composites based on electrostatic theory that satisfies the Laplace equation (Ref 12, 13). In this model, there are n spheres of radius r_1 and resistance ρ_p placed into a larger sphere of radius r_2. These spheres are at such distances that they do not interact and can be taken as independent of each other. Furthermore, this larger sphere is placed into an infinitely extended homogenous medium whose resistance is ρ_m. The ratio of the volume (p) of the smaller spheres (r_1) to that of the larger sphere (r_2) that contains them is:

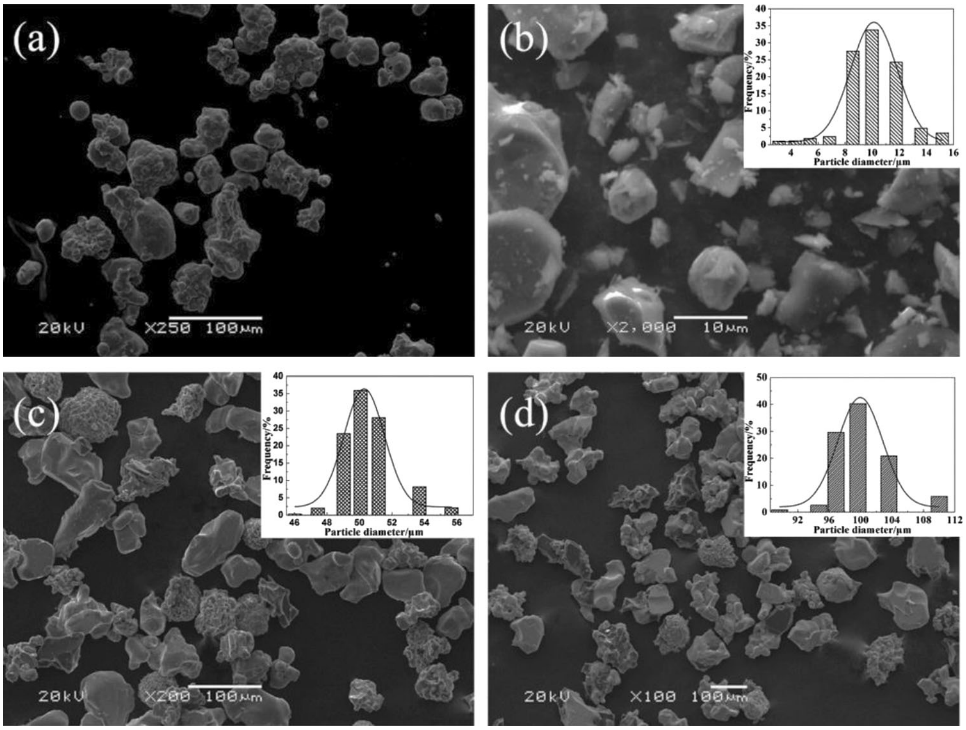

Fig. 1 SEM micrographs of the original powders: (a) 75 μm Cu powder; (b) 10 μm TiB_2 powder; (c) 50 μm TiB_2 powder; (d) 100 μm TiB_2 powder

$$p = \frac{nr_1^3}{r_2^3} \qquad \text{(Eq 1)}$$

The potential that a large distance from the center of this sphere will be of the following form is:

$$V_1 = -E_0 R\cos\theta + p\frac{\rho_\mathrm{p} - \rho_\mathrm{m}}{2\rho_\mathrm{p} + \rho_\mathrm{m}} \cdot \frac{E_0 r_2^3}{R^2}\cos\theta \qquad \text{(Eq 2)}$$

Now, if the entire sphere of radius r_2 and resistance ρ_Maxwell is considered, the equation becomes:

$$V_2 = -E_0 R\cos\theta + \frac{\rho_\mathrm{Maxwell} - \rho_\mathrm{m}}{2\rho_\mathrm{Maxwell} + \rho_\mathrm{m}} \cdot \frac{E_0 r_2^3}{R^2}\cos\theta \qquad \text{(Eq 3)}$$

The far-field potential is indicated by $V_1 = V_2$; therefore, the resistance of the composite is obtained by:

$$\rho_\mathrm{Maxwell} = \frac{2\rho_\mathrm{p} + \rho_\mathrm{m} + p(\rho_\mathrm{p} - \rho_\mathrm{m})}{2\rho_\mathrm{p} + \rho_\mathrm{m} - 2p(\rho_\mathrm{p} - \rho_\mathrm{m})} \cdot \rho_\mathrm{m} \qquad \text{(Eq 4)}$$

Since electrical conductivity σ is equal to $1/\rho$, the electrical conductivity of the composites can be obtained by:

$$\sigma_\mathrm{Maxwell} = \frac{\sigma_p + 2\sigma_m + 2p(\sigma_p - \sigma_m)}{\sigma_p + 2\sigma_m - p(\sigma_p - \sigma_m)} \cdot \sigma_m \qquad \text{(Eq 5)}$$

According to Eq 3, the particle volume fraction (p) is determined by the selection of n, r_1, and r_2. If n and r_1 are fixed, the arbitrary selection of r_2 can yield an infinite number of ps, while Eq 5 calculates the corresponding σ_Maxwell. If r_2 and p are fixed, when n is modified, r_1 will also change. However, according to Eq 5, regardless of n, r_1 for the electrical conductivity calculation remains constant. Therefore, the Maxwell equation takes into account the influence of the volume fraction on the conductivity, while the size of the particles is not reflected in the equation.

The lattice of an ideal metal has a strict periodicity, and the electrons move in the periodic equivalent potential field. According to the Schrödinger equation for ideal metals, electron motion has a nonzero velocity and does not decelerate due to collision. For ideal crystals, the conductivity is infinite. A sphere placed in an infinitely extended homogenous medium, which destroys the periodic potential field, will result in electron scattering. Therefore, when p and r_2 are constant, n is greater, r_1 is smaller, and electron scattering increases, the electrical conductivity decreases.

According to the Drude model of electron theory, the relationship between the electrical conductivity and electron mean free path is given by (Ref 19):

$$\frac{\sigma}{\mathrm{mfpe}} = \text{constant} \qquad \text{(Eq 6)}$$

where mfpe is the mean free path for electron conductivity and σ is the electrical conductivity. The mfpe of pure copper is a constant (approximately 42 nm); however, when the particles are introduced into the pure copper matrix, the mfpe is reduced. However, nearly all of the existing models express electrical conductivity of composites in terms of volume fractions, which results in deviations between the predicted and experimental values. The volume fraction of the particle strongly influences the electrical conductivity of the composite; however, the particle size and interface also have strong effect on the electrical conductivity. The particle spacing affects the electronic mean free path of composites, which in turn affects the electrical conductivity of the composites. The particle spacing is determined by the volume fraction and size of the particles, which can be calculated by Eq 9. Thus, based on the Maxwell

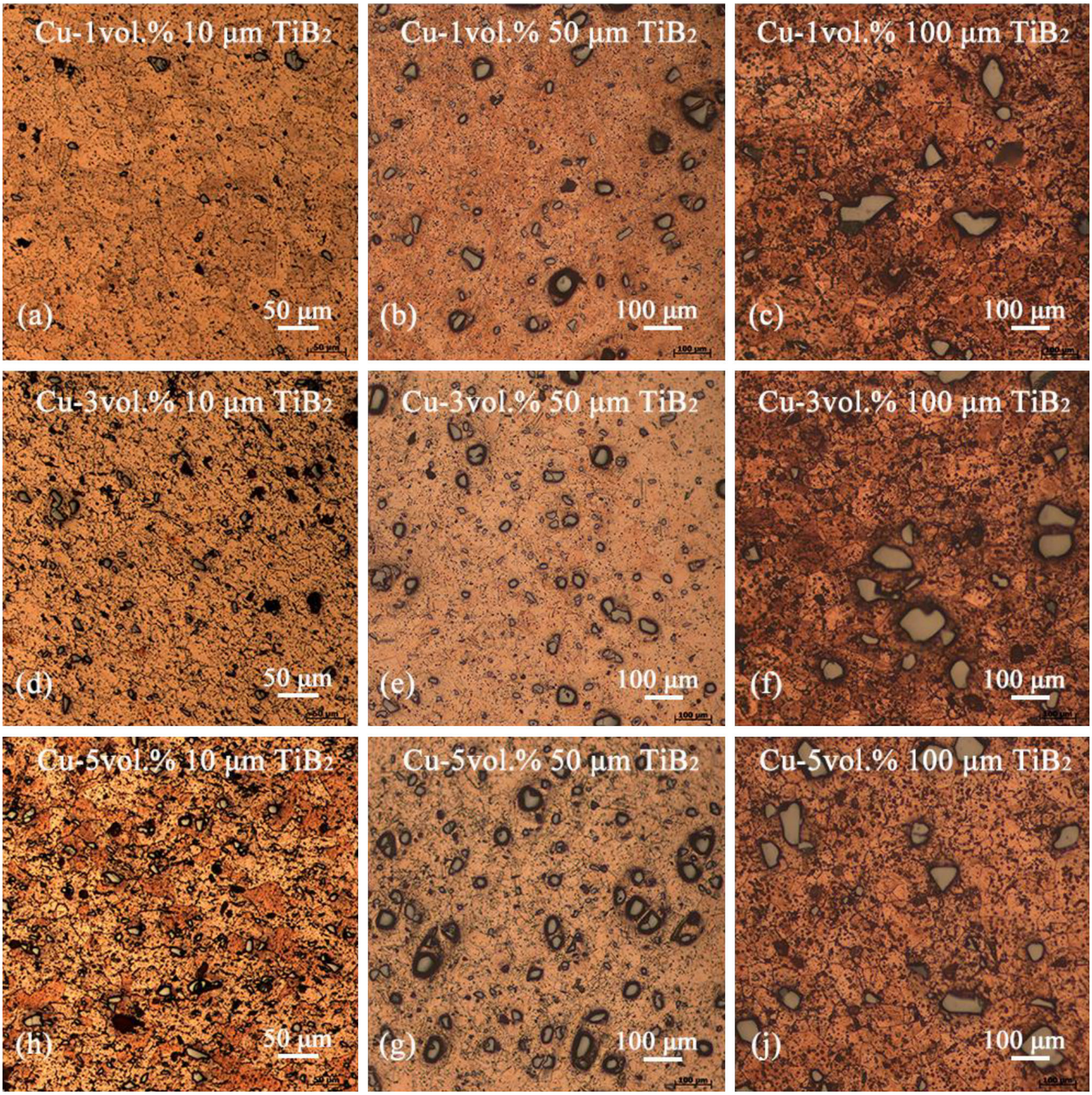

Fig. 2 Optical micrographs of TiB_2/Cu composites reinforced with various volume fractions and particle sizes of TiB_2

model, the dimensionless particle spacing parameter equation $g(L)$ is introduced to describe the effect of the particle size and interface on the electrical conductivity of composites. The dimensionless particle spacing parameter is suggested to be established by the volume fraction (p), particle size (d), and interfacial factor (a). This equation is derived as follows:

$$\sigma = (1 - g(L)) \cdot \sigma_{\mathrm{Maxwell}} \qquad \text{(Eq 7)}$$

$$\mathrm{g}(L) = \frac{a \cdot \ln(42)}{\ln(L)} \qquad \text{(Eq 8)}$$

$$L = \left(\frac{2\pi}{3p}\right)^{1/2} \cdot \left(\frac{d}{2}\right) \qquad \text{(Eq 9)}$$

where a is the particle–matrix interfacial factor and d is the particle diameter. By substituting Eq 8 and 9 into Eq 7, the following equation for the electrical conductivity of composites is derived:

$$\sigma = \left(1 - \frac{a \cdot \ln(42)}{\ln\left[\left(\frac{2\pi}{3p}\right)^{1/2} \cdot \left(\frac{d}{2}\right)\right]}\right) \cdot \sigma_{\mathrm{Maxwell}} \qquad \text{(Eq 10)}$$

For a constant a, the theoretical electrical conductivity ($\sigma_{\mathrm{Maxwell}}$) of the TiB_2/Cu composites is taken with the volume fraction of 1%, 3%, or 5%. The value of a can be calculated using Eq 5; experimental data (σ), particle size (d), and volume fraction (p) from Table 1; Eq 8 and 9; and the electrical

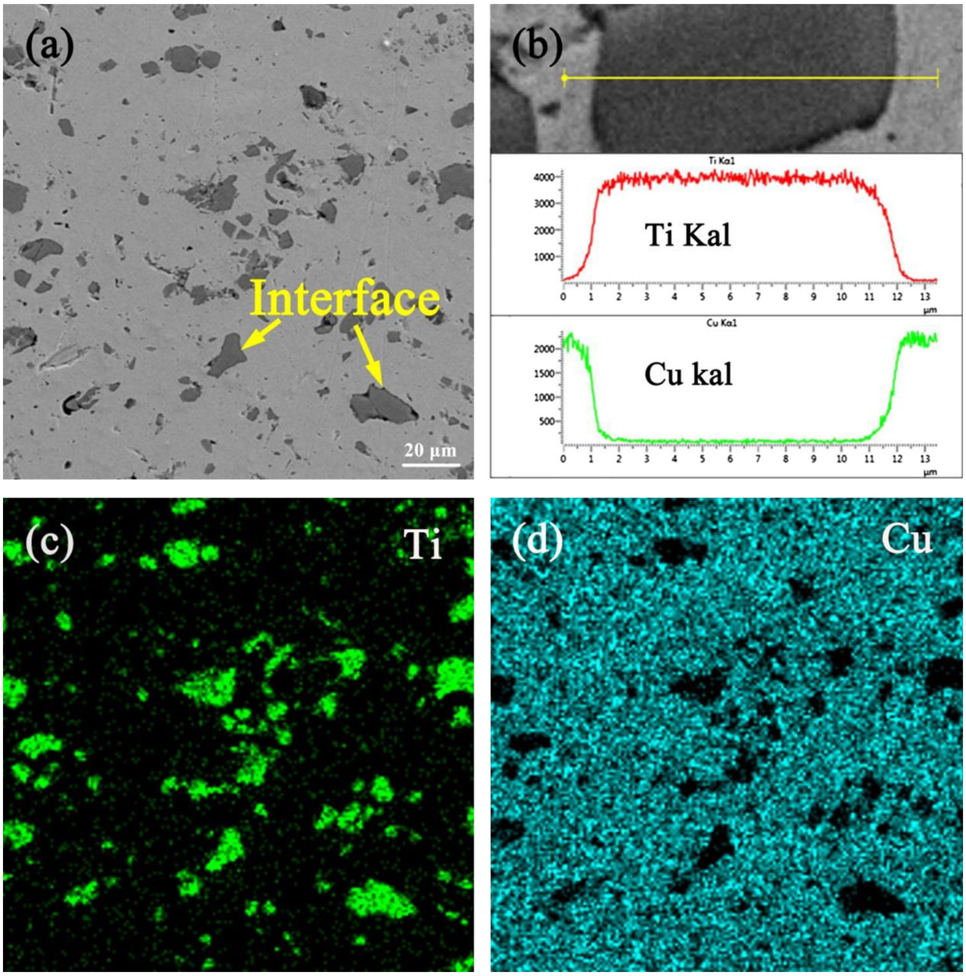

Fig. 3 SEM images, corresponding EDS maps, and element line scans of Cu-5 vol. % 10 µm TiB2 composite

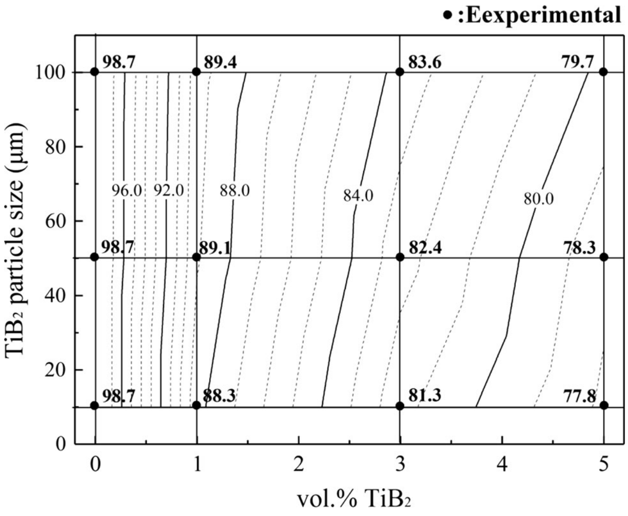

Fig. 4 Electrical conductivity (% IACS) contour diagram of TiB_2/Cu composites as a function of TiB_2 particle size and volume fraction

conductivities of TiB_2 (σ_p = 11.97% IACS) and copper (σ_m = 100% IACS). These data are then substituted into Eq 10:

Then,

$$a = \left(1 - \frac{\sigma}{\sigma_{\text{Maxwell}}}\right) \cdot \ln\left[\left(\frac{2\pi}{3p}\right)^{1/2} \cdot \left(\frac{d}{2}\right)\right] \bigg/ \ln(42) \qquad \text{(Eq 11)}$$

According to Eq 11, the a_i value was calculated using the volume fraction and particle size of TiB_2/Cu composites, as given in Table 1. The results in Table 1 illustrate that the particle–matrix interfacial factor (a) of each composite is different. Since the TiB_2 particles are irregular spherical shapes, they do not assume an ideal uniform distribution in the matrix. Therefore, a must be determined by averaging the values.

The mean a values were obtained by fitting the electrical conductivity of 10 µm, 50 µm, and 100 µm TiB_2/Cu samples of different volumes (%) from Table 1, wherein a = 0.43. By substituting a = 0.43 into Eq 10, we derive the electrical conductivity prediction model of the copper matrix composites as:

$$\sigma = \left(1 - \frac{1.61}{\ln\left[\left(\frac{2\pi}{3p}\right)^{1/2} \cdot \left(\frac{d}{2}\right)\right]}\right) \cdot \sigma_{\text{Maxwell}} \qquad \text{(Eq 12)}$$

The electrical conductivity of the ceramic particles is significantly less than that of copper, which is almost zero. Consequently, Eq 12 can be simplified to Eq 13.

Table 1 Experimental parameters of TiB_2/Cu composites

Samples no.	TiB_2/Cu composite	Experimental data, % IACS	a_i	Maxwell model, % IACS	Modified model, % IACS
1	10 µm-1 vol. %	88.3	0.32	98.8	84.5
2	10 µm-3 vol. %	81.3	0.44	96.3	81.7
3	10 µm-5 vol. %	77.8	0.48	93.9	79.3
4	50 µm-1 vol. %	89.1	0.33	98.8	86.3
5	50 µm-3 vol. %	82.4	0.47	96.3	83.7
6	50 µm-5 vol. %	78.3	0.53	93.9	81.3
7	100 µm-1 vol. %	89.4	0.34	98.8	87.0
8	100 µm-3 vol. %	83.6	0.46	96.3	84.3
9	100 µm-5 vol. %	79.7	0.51	93.9	82.0

$$\sigma = \left(1 - \frac{1.61}{\ln\left[\left(\frac{2\pi}{3p}\right)^{1/2} \cdot \left(\frac{d}{2}\right)\right]}\right) \cdot \frac{2-2p}{2+p} \cdot \sigma_{\mathrm{m}} \qquad \text{(Eq 13)}$$

Equation 12 and 13 are deduced on the basis of the Maxwell equation, where the particles are assumed to be spherical and the volume fraction is less than 15%. Thus, Eq 12 and 13 are only applied to predict the conductivity of the spherical-particle-reinforced copper matrix composites.

The modified model was compared with the Maxwell equation, and the results of the prediction are given in Table 1. We agree that the influence of particle size on the electrical conductivity of the copper matrix composites should be considered. Here, we focused mainly on the effect of the volume fraction and particle size on the electrical conductivity. We further increased the precision of our model compared with that of other prediction models.

The electrical conductivity under different volume fractions and particle sizes can be predicted using Eq 12, as shown in Fig. 5. The electrical conductivity can more intuitively be determined by the volume fraction and particle size. As observed in Fig. 5, when the particle size is on the nanoscale, the electrical conductivity of the copper matrix composite is predominantly affected by the particle size. However, when the particle size is on the micron range, the electrical conductivity of the copper matrix composites is more so affected by the volume fraction.

To verify the modified model, the predicted modified model data were compared with the experimental data reported in Ref 24 (Table 2). The comparison shows that the modified model prediction can be used to predict the electrical conductivity of the copper matrix composites. As such, particle size is an important factor to consider. Efe et al. (Ref 1) studied the effect of SiC particle size on the electrical conduction of SiC/Cu composites. The data of the modified model prediction agree with the experimental data displayed in Table 2.

3.4 Effect of the Interfacial Bonding State on the Electrical Conductivity

The main factors affecting the electrical conductivity of the particle-reinforced copper matrix composites include the volume fraction, particle size, distribution, and the interfacial bonding state between the particles and the copper matrix. Copper matrix composites can be prepared by ex situ or in situ synthesis. Although the ex situ method can easily control the particle size, the interface bonding state is often ignored. Comparatively, in situ synthesis can improve the interface bonding state; however, maintaining a uniform particle size (all nanometers, submicron or microns) is extremely difficult. Therefore, under the assumption that the interfacial bonding state is reasonable, we investigated the effect of the volume fraction and particle size on the electrical conductivity of an ex situ synthesized copper matrix composite.

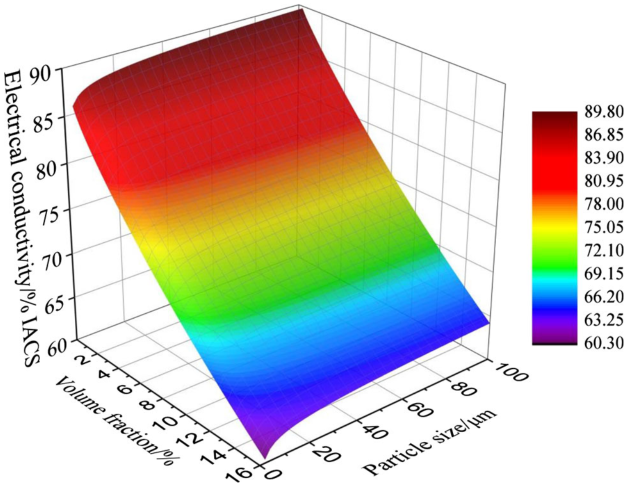

Fig. 5 Dependence of electrical conductivity on volume fraction and size of TiB_2 particles

The modified model was further verified, as was the effect of interfacial factors on electrical conductivity. Our research group has recently studied the effect of the interface bonding state of MgO_p/Cu composites on their electrical conductivity (Ref 24). Figure 6 displays the morphology of the MgO particles in the 1.0 vol. % MgO_p/Cu composite fabricated by ex situ and in situ methods, respectively. Here, the black MgO particles are uniformly distributed in the copper matrix. The interface between MgO_p and the Cu matrix of the MgO_p/Cu composite prepared by ex situ synthesis is incoherent, similar to that of the TiB_2/Cu composites prepared by ex situ synthesis. Thus, the interfaces of the MgO_p/Cu composite prepared by in situ synthesis possess semicoherent interfaces and a crystallographic orientation relationship between the MgO_p and Cu matrix. The electrical conductivity of the two composites was 75.1% IACS and 88.2% IACS, respectively. The electrical conductivity predicted for the two composites by Eq 13 is 71.6% IACS and 58.8% IACS. These results indicate that Eq 13 can predict the electrical conductivity of the MgO_p/Cu

Table 2 Comparison of the present model with the experimental data reported in Ref 1, 6, 23-27

Preparation	Composite	Particle size, nm	Experimental data, % IACS	Modified model, % IACS	Error, % IACS	Ref
Ex situ	Cu-5.36 vol. % SiC	1000	76.7	73.7	− 3	Ref 1)
Ex situ	Cu-7.90 vol. % SiC	1000	66.6	70.4	3.8	Ref 1)
Ex situ	Cu-5.36 vol. % SiC	5000	82.9	76.8	− 6.1	Ref 1)
Ex situ	Cu-7.90 vol. % SiC	5000	77.3	73.5	− 3.8	Ref 1)
Ex situ	Cu-1 vol. % MgO	50	75.1	71.6	− 3.5	Ref 24)
In situ	Cu-1 vol. % MgO	5-10	88.2	88.4	0.2	Ref 24)
In situ	Cu-1.94 vol. % TiB_2	400-900	87.2	91.1	3.9	Ref 6)
In situ	Cu-0.5 vol. % Al_2O_3	20-50	93.0	92.3	− 0.7	Ref 25)
In situ	Cu-0.54 vol. % Al_2O_3	18	93.0	91.3	− 1.7	Ref 26)
In situ	Cu-1.53 vol. % ZrB_2	5000	94.1	93.8	− 0.3	Ref 22)
In situ	Cu-0.91vol. % Cr	10-20	90.8	90.3	− 0.5	Ref 27)
In situ	Cu-1.53 vol. % ZrB_2	200	89	92	3	Ref 23)

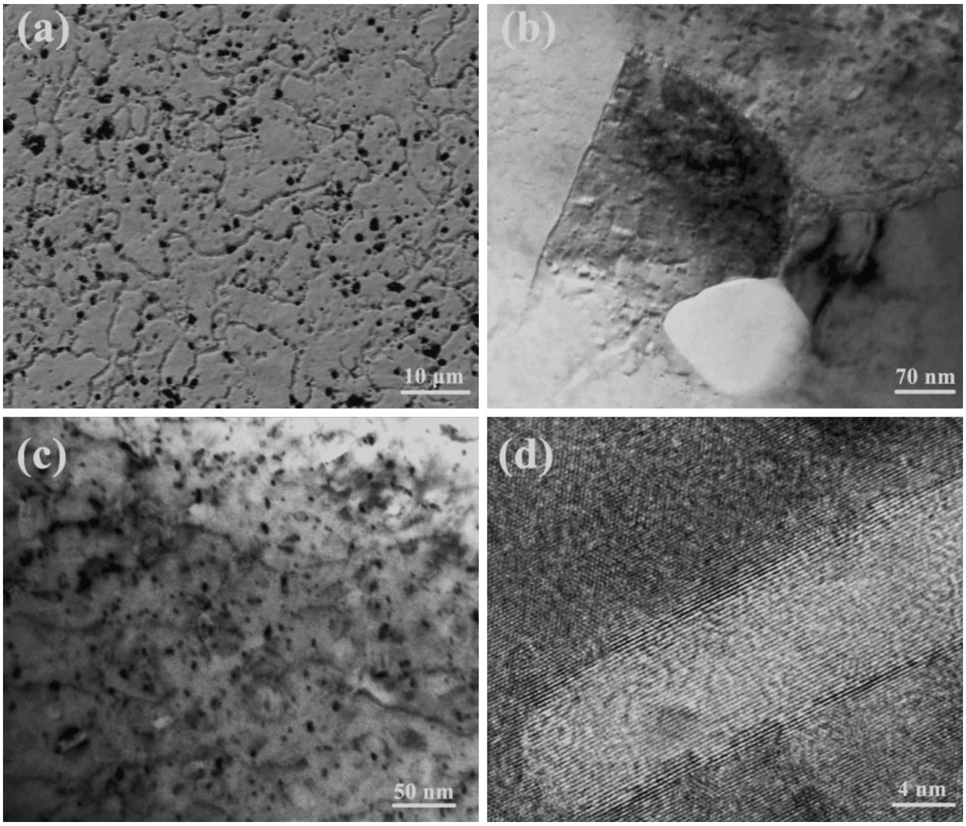

Fig. 6 Morphology of the MgO particles in the 1.0 vol. % MgO_p/Cu composite fabricated by ex situ (a, b) and in situ (c, d) synthesis, respectively (Ref 24)

composites prepared by ex situ synthesis but not the conductivity of those prepared by in situ synthesis.

According to the theory of solid physical metal electrons, the ideal crystal lattice has no scattering effect on the electrons. When the lattice orientation at the interface between the particle and matrix is consistent, the effect of the interface on the electrical conductivity is negligible. When the interface bonding state between the particles and matrix is coherent or semicoherent, the lattice orientation of the interface tends to be consistent. This process decreases the lattice distortion of the matrix and interfacial resistivity; otherwise, the interfacial resistivity would increase. Therefore, when the interface between the particles and copper matrix is incoherent, the interfacial factor a = 0.43. When the interface is coherent or semicoherent, in accordance with the experimental data in Ref 24 and Eq 11, the interfacial factor a = 0.11, which is lower than the interfacial factor (*a*) of an incoherent. Thus, a coherent or semicoherent interfacial bonding state exhibits weaker electron scattering and improves the electrical conductivity of the composites. Comparisons between model predictions and experimental data reported in Ref 1, 6, 23-27 are given in Table 2. When the volume fraction, particle size, distribution, and interface are considered, the modified model predicts the electrical conduction of the copper matrix composites well and the error is very small.

4. Conclusion

Experimental and theoretical analyses have revealed that the particle size, volume fraction and interfacial bonding state are key parameters that influence the electrical conductivity of composites. The electrical conductivity of copper matrix composites decreases with increasing particle volume fraction and increases with increasing particle size. Therefore, particle size should be considered in the predictive models. The modified model was established based on the Maxwell model, which is in accordance with the experimental data reported in the literature. In this regard, particle size is a necessary element for calculating the electrical conductivity.

Acknowledgments

This work was supported by the National Natural Science Foundation of China (Grant Nos. U1502274 and 51605146), China Postdoctoral Science Foundation (No.2018M632769), and Henan Plan Project for College Youth Backbone Teacher (2018GGJS045).

References

1. G.C. Efe, M. Ipek, S. Zeytin, and C. Bindal, An Investigation of the Effect of SiC Particle Size on Cu-SiC Composites, *Compos. Part B*, 2012, **4**, p 1813–1822
2. L.Y. Gu, G.Y. Liang, and Z.B. Zheng, Investigation of in Situ Cu-TiB_2 Composite on the Copper Using Laser Melting Synthesis, *J. Mater. Eng. Perform.*, 2007, **16**, p 554–558
3. K.M. Liu, Z.X. Wang, Z.Y. Jiang, A. Atrens, Z.K. Huang, X.G. Zhang, W. Guo, X.W. Zhang, J.M. Yu, Q.G. Lu, and D.P. Lu, Cu-7Cr-0.1Ag Microcomposites Optimized for High Strength and High Condutivity, *J. Mater. Eng. Perform.*, 2018, **27**, p 1–6
4. A. Fathy and O. El-Kady, Thermal Expansion and Thermal Conductivity Characteristics of Cu-Al_2O_3 Nanocomposites, *Mater. Des.*, 2013, **46**, p 355–359
5. A. Fathy, Investigation on Microstructure and Properties of Cu-ZrO_2 Nanocomposites Synthesized by in Situ Processing, *Mater. Lett.*, 2018, **213**, p 95–99
6. C.L. Zou, H.J. Kang, W. Wang, Z.N. Chen, R.G. Li, X.X. Gao, T.J. Li, and T.M. Wang, Effect of La Addition on the Particle Characteristics, Mechanical and Electrical Properties of in Situ Cu-TiB_2 Composites, *J. Alloys Compd.*, 2016, **687**, p 312–319
7. G.A. Bagheri, The Effect of Reinforcement Percentages on Properties of Copper Matrix Composites Reinforced with TiC Particles, *J. Alloys Compd.*, 2016, **676**, p 120–126
8. K.X. Song, P. Liu, B.H. Tian, Q.M. Dong, and J.D. Xing, Stabilization of Nano-Al_2O_{3p}/Cu Composite after High Temperature Annealing Treatment, *Mater. Sci. Forum*, 2005, **475–479**, p 993–996
9. J.P. Tu, N.Y. Wang, Y.Z. Yang, W.X. Qi, F. Liu, X.B. Zhang, H.M. Lu, and M.S. Liu, Preparation and Properties of TiB_2, Nanoparticle Reinforced Copper Matrix Composites by in Situ Processing, *Mater. Lett.*, 2002, **52**, p 448–452
10. A. Fathy, O. Elkady, and A. Abu-Oqail, Synthesis and Characterization of Cu-ZrO_2 Nanocomposite Produced by Thermochemical Process, *J. Alloys Compd.*, 2017, **719**, p 411–419
11. A. Fathy, O. Elkady, and A. Abu-Oqail, Production and Properties of Cu-ZrO_2 Nanocomposites, *J. Compos. Mater.*, 2018, **52**, p 1519–1529
12. J.C. Maxwell, *A Treatise on Electricity and Magnetism*, Clarendon Press, Oxford, 1881
13. J.Z. Xu, B.Z. Gao, and F.Y. Kang, A Reconstruction of Maxwell Model for Effective Thermal Conductivity of Composite Materials, *Appl. Therm. Eng.*, 2016, **102**, p 972–979
14. L. Rolf, The Electrical Resistance of Binary Metallic Mixtures, *J. Appl. Phys.*, 1952, **23**, p 779–784
15. F.S. Roig and J.E. Schoutens, Remarks on the Use of Boltzmann's Equation for Electrical Conduction Calculations in Metal Matrix and in Situ Composites, *J. Mater. Sci.*, 1986, **21**, p 2767–2770
16. F.S. Roig and J.E. Schoutens, Theory of Electrical Resistivity of Metal-matrix Composites at Cryogenic and Higher Temperatures, *J. Mater. Sci.*, 1986, **21**, p 2409–2417
17. J.E. Schoutens and F.S. Roig, Model of Transverse Electrical Conductivity of Metal Matrix Composites above Liquid Nitrogen Temperatures, *J. Mater. Sci.*, 1987, **22**, p 181–188
18. R. Pal, On the Lewis–Nielsen Model for Thermal/Electrical Conductivity of Composites, *Compos. Part A*, 2008, **39**, p 718–726
19. F. Heringhaus, H.J. Schneider-Muntau, and G. Gottstein, Analytical Modeling of the Electrical Conductivity of Metal Matrix Composites: application to Ag-Cu and Cu-Nb, *Mater. Sci. Eng. A*, 2003, **347**, p 9–20
20. Z. Hashin, Assessment of the Self Consistent Scheme Approximation: conductivity of Particulate Composites, *J. Compos. Mater.*, 1968, **2**, p 284–300
21. R.F. Jones and B. Roebuck, The Relation Between Electrical Resistivity and Particulate Volume Fraction in Aluminium Alloy Metal-matrix Composites, *J. Mater. Sci. Lett.*, 1989, **8**, p 573–575
22. Z.G. Zhang, Y.Y. Sheng, X. Xu, and W. Li, Microstructural Features and Mechanical Properties of In Situ Formed ZrB_2/Cu Composites, *Adv. Eng. Mater.*, 2015, **17**, p 1338–1343
23. C. Wang, H.J. Lin, Z. Zhang, and W. Li, Fabrication, Interfacial Characteristics and Strengthening Mechanisms of ZrB_2, Microparticles Reinforced Cu Composites Prepared by Hot-pressed Sintering, *J. Alloys Compd.*, 2018, **748**, p 546–552
24. X.H. Guo, K.X. Song, S.H. Liang, Y.J. Zhou, and X. Wang, Relationship Between the MgO_p/Cu Interfacial Bonding State and the Arc Erosion Resistance of MgO/Cu Composites, *J. Mater. Res.*, 2017, **32**, p 3753–3760
25. B.H. Tian, P. Liu, K.X. Song, Y. Li, Y. Liu, F.Z. Ren, and J.H. Sun, Microstructure and properties at Elevated Temperature of a Nano-Al_2O_3 Particles Dispersion-strengthened Copper Base Composite, *Mater. Sci. Eng. A*, 2006, **435–436**, p 705–710
26. J.Y. Cheng, M.P. Wang, Z. Li, C.W. Xiao, and B. Hong, Fabrication and Properties of Low Oxygen Grade Al_2O_3 Dispersion Strengthened Copper Alloy, *Trans. Nonferr. Met. Soc. China.*, 2004, **14**, p 121–126
27. L.J. Peng, H.F. Xie, G.J. Huang, G.L. Xu, X.Q. Yin, X. Feng, X.J. Mi, and Z. Yang, The Phase Transformation and Strengthening of a Cu-0.71wt% Cr Alloy, *J. Alloys Compd.*, 2017, **708**, p 1096–1102